JACS
JOURNAL OF THE AMERICAN CHEMICAL SOCIETY
Article
pubs.acs.org/JACS

Enantiospecific *cis*–*trans* Isomerization in Chiral Fulleropyrrolidines: Hydrogen-Bonding Assistance in the Carbanion Stabilization in $H_2O@C_{60}$

Enrique E. Maroto,[†] Jaime Mateos,[†] Marc Garcia-Borràs,[§] Sílvia Osuna,*[,§] Salvatore Filippone,*[,†] María Ángeles Herranz,[†] Yasujiro Murata,[∥] Miquel Solà,*[,§] and Nazario Martín*[,†,‡]

[†]Departamento de Química Orgánica I, Facultad de Química, Universidad Complutense, E-28040 Madrid, Spain
[‡]Nanoscience, Campus de Cantoblanco, IMDEA, E-28049 Madrid, Spain
[§]Institut de Química Computacional i Catàlisi (IQCC) and Departament de Química, Universitat de Girona, 17071 Girona, Spain
[∥]Institute for Chemical Research, Kyoto University, Uji, Kyoto 611-0011, Japan

Supporting Information

ABSTRACT: The stereochemical outcome of *cis*–*trans* isomerization of optically pure [60], [70], and endohedral $H_2O@C_{60}$ fulleropyrrolidines reveals that the electronic nature of substituents, fullerene size, and surprisingly the incarcerated water molecule plays a crucial role in this rearrangement process. Theoretical DFT calculations are in very good agreement with the experimental findings. On the basis of the experimental results and computational calculations, a plausible reaction mechanism involving the hydrogen-bonding assistance of the inner water molecule in the carbanion stabilization of endofullerene is proposed.

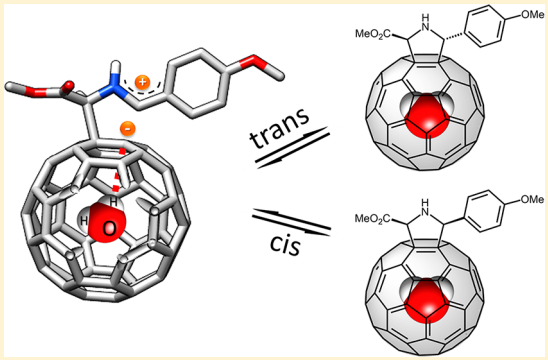

INTRODUCTION

Rearrangement and retrocycloaddition processes on fullerenes have attracted much attention since they reveal the amazing reactivity of these highly strained curved molecules.[1] Rearrangements are especially valuable as they constitute an effective way of broadening the structural wealth, thus increasing the diversity and variety of fullerene derivatives. In this regard, thermal and photochemical fulleroid-methanofullerene conversions via di-π-methane (Zimmerman) rearrangements are typical and known since the early days of fullerenes.[2] Electrochemically induced "walking on the sphere" of Bingel cycloadducts[3] as well as the unusual migration from [6,6]- to [5,6]-junction on some endohedral[4] and aziridinofullerenes[5] have also been reported. On the other hand, cyclic functional groups rearrangements on fullerenes are closely related to the retrocycloaddition processes.[6] Thus, fullerene derivatives can, under certain conditions, undergo kinetically controlled retrocycloaddition reactions that have proven their worth in several protection–deprotection protocols.[6c,d] However, despite the interest of the aforementioned chemical transformations, their stereochemical studies have not been properly addressed and still remain as a significant scientific demanding task.

In this regard, endohedral fullerenes having a chemical species in the inner cavity of fullerene represent a valuable and a singular scenario where the encapsulated species can contribute to the chemical transformation, thus providing further mechanistic information.

As a representative example, it has recently been reported that the strong impact of the incarcerated lithium cation in $[Li^+@C_{60}](PF_6^-)$ in the Diels–Alder reaction is due to the lowering of the LUMO level of the fullerene double bond by interacting with the Li^+.[7]

Chiral information is a valuable tool to inquire into mechanistic aspects. However, a major obstacle toward the use of stereochemical studies has been the scarce availability of chiral starting fullerenes. In this regard, we have recently reported a highly efficient methodology to obtain enantiomerically enriched fullerene derivatives with a total stereochemical control by means of either metallic catalysts[8] or organocatalysts.[9]

Herein, we report the first *cis*–*trans* isomerization reaction from enantiomerically enriched fullerene derivatives. The experimental findings and theoretical DFT calculations reveal that this process operates on a completely stereospecific manner.

Furthermore, the *cis*–*trans* isomerization also works efficiently in the less-explored endohedral fullerenes, namely $H_2O@C_{60}$. Interestingly, we report on an unprecedented

Received: October 23, 2014
Published: January 5, 2015

DOI: 10.1021/ja5108854
J. Am. Chem. Soc. 2015, 137, 1190–1197

behavior of the inner water molecule in assisting the stabilization of the carbanion formed during the isomerization process through hydrogen-bonding (H-bonding) involving a water H atom.

Making use of optically pure cycloadducts as stereochemical tools, the study of the isomerization process has been carried out considering three different levels (Figure 1): (i) [60]-

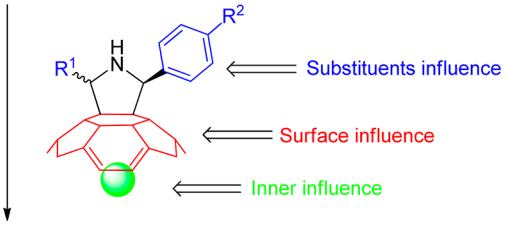

Figure 1. "Three level" approach that may influence the stereochemical result of the *cis*–*trans* isomerization in fulleropyrrolidines.

fullerene is a symmetric π-system scenario where the isomerization could only be influenced by variations in the exohedral substituents located on the sphere; (ii) changing into [70]fullerene adds new carbon atoms with different reactivity due to the loss of symmetry, but still maintaining an exohedral activity in the fullerene surface; and (iii) the presence of chemical species in the inner cavity of the fullerene cage might affect the isomerization process and/or the kinetic and the stereochemical result.

RESULTS AND DISCUSSION

Synthesis of Enantiomerically Enriched Starting Materials. The series of chiral metal–ligand pairs and bases, already reported by our group,[8] achieved a total stereodivergent control in the 1,3-dipolar cycloaddition of N-metalated azomethine ylides onto fullerenes under mild conditions. Thus, enantiomerically enriched 2-methoxycarbonyl-5-aryl substituted pyrrolidino[60]fullerenes (**2a–e**) and [70]-fullerenes (**3** and **4**) in all their stereoisomeric variants were synthesized with optical purities in the range of 80–99% (Figure 2; see also Supporting Information (SI)).

In order to determine an eventual effect of the incarcerated polar molecule inside the fullerene sphere, we have carried out the synthesis of unprecedented enantiomerically enriched endohedral fulleropyrrolidines **5a** with an inner water molecule, by means of the cycloaddition of α-iminoester **1a** onto the asymmetric endofullerene $H_2O@C_{60}$.[10] Our previously described methodology for the catalytic stereodivergent functionalization of endohedral fullerenes[11] afforded *cis* and *trans* $H_2O@C_{60}$ cycloadducts **5a** with excellent asymmetric induction results (Scheme 1).

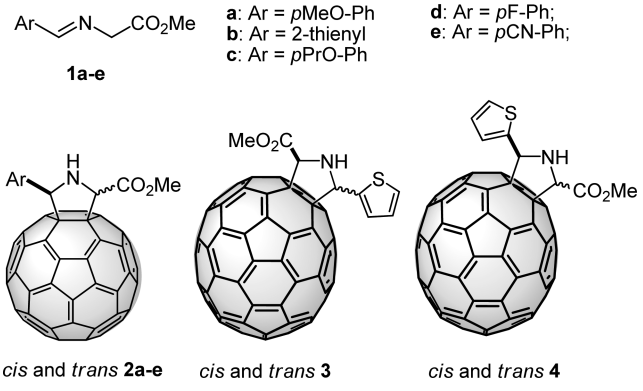

Figure 2. Optically enriched [60] and [70]fulleropyrrolidines.

Scheme 1. Stereodivergent Synthesis of the Four Stereoisomers of the Endohedral Water-Encapsulating Fulleropyrrolidines 5a

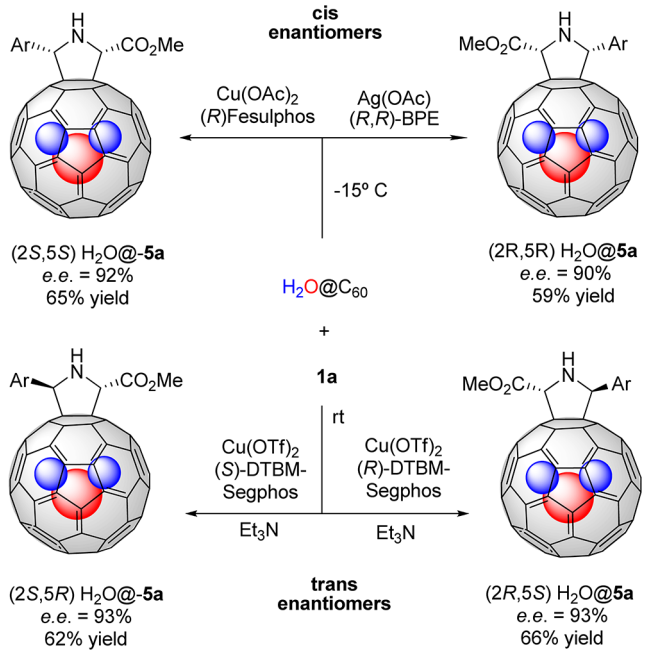

Screening and Optimal Conditions for the Isomerization. To study the viability of the process, we chose as a model reaction the isomerization of (2*S*,5*S*)-*cis* pyrrolidinofullerene **2a** into the *trans* adduct. Different reaction parameters, such as solvent polarity and temperature, were screened to find suitable conditions for the rearrangement process in high yield and with high stereospecificity (Table 1).

Fortunately, *cis*-**2a** underwent isomerization reaction into the *trans* diastereoisomer. The reaction reached an equilibrium state where a mixture of both *cis* and *trans*-**2a** adducts was present in a 7:3 concentration relationship. Surprisingly, *cis* isomer was the major and thermodynamically controlled product (*vide infra*).

Among the tested conditions, solvent mixtures of 1-chloronaphthalene:acetonitrile and toluene:acetonitrile both in 1:10 ratio, afforded at 35 °C the best outcome. Pleasingly, (2*S*,5*S*)-*cis* enantiomer isomerized exclusively into the (2*S*,5*R*)-*trans* adduct and maintained the same optical purity as the starting material (Table 1, entries 10–11). These unprecedented results led us to test the behavior of the opposite (2*R*,5*R*) enantiomer under the same conditions, that converted after 6 days into the contrary (2*R*,5*S*)-*trans* isomer with identical degree of enantiospecificity (Table 1, entry 12). To better illustrate the results, 99% optically pure enantiomers of *cis*-**2a** were prepared by chiral HPLC separation, furnishing totally enantiospecific isomerization profiles with up to 97% of enantiomeric excess (ee) in the new formed *trans* adduct (Table 1, entry 13).

The reaction was effectively reversible, affording equal equilibrium results when using (2*S*,5*R*)-*trans*-**2a** as chiral starting material (Table 1, entry 14). It is important to remark

DOI: 10.1021/ja5108854
J. Am. Chem. Soc. 2015, 137, 1190–1197

Table 1. Representative Results for the Screening of Reaction Conditions for the Isomerization of (2*S*,5*S*)-*cis*-2a

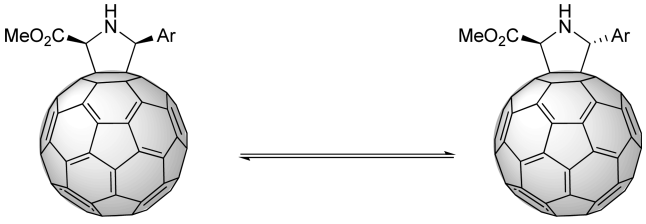

entry	solvent[a]	*t* (d)	*T* (°C)	*cis*:*trans*[b]	ee *cis*(%)[c]	ee *trans*(%)[c]
1	–	0	–	99:1	92 (2*S*,5*S*)	–
2	toluene	20	50	73:27	35 (2*S*,5*S*)	47 (2*S*,5*R*)
3	toluene	25	35	87:13	61 (2*S*,5*S*)	65 (2*S*,5*R*)
4	MeOH	40	50	92:8	65 (2*S*,5*S*)	–
5	Tol/MeOH	40	50	83:17	64 (2*S*,5*S*)	60 (2*S*,5*R*)
6	MeCN	40	50	70:30	72 (2*S*,5*S*)	70 (2*S*,5*R*)
7	Cl-Nap/MeCN	5	50	70:30	81 (2*S*,5*S*)	80 (2*S*,5*R*)
8	Tol/MeCN	8	50	70:30	70 (2*S*,5*S*)	70 (2*S*,5*R*)
9	Cl-Nap/MeCN	25	20	75:25	87 (2*S*,5*S*)	87 (2*S*,5*R*)
10	Cl-Nap/MeCN	6	35	72:28	90 (2*S*,5*S*)	90 (2*S*,5*R*)
11	Tol/MeCN	9	35	71:29	89 (2*S*,5*S*)	89 (2*S*,5*R*)
12[d]	Cl-Nap/MeCN	6	35	66:34	88 (2*R*,5*R*)	88 (2*R*,5*S*)
13[e]	Cl-Nap/MeCN	6	35	72:28	97 (2*S*,5*S*)	97 (2*S*,5*R*)
14[f]	Cl-Nap/MeCN	6	35	70:30	93 (2*S*,5*S*)	93 (2*S*,5*R*)

[a]Solvent mixtures ratios are 1/10. [b]Diastereoisomers ratio determined by HPLC (see SI). [c]Enantiomeric excesses (ee) measured by chiral HPLC. [d](2*R*,5*R*)-*cis* pyrrolidinofullerene **2a** (90% optical purity) employed as starting material. [e](2*S*,5*S*)-*cis* pyrrolidinofullerene **2a** (99% optical purity) employed as starting material. [f](2*S*,5*R*)-*trans* pyrrolidinofullerene **2a** (95% optical purity) employed as starting material.

that the absolute configuration of the pyrrolidine carbon C2 (Scheme 2) is retained in every *cis*−*trans* diastereoisomer interconversion.

Low polarity and solubility resulted in too long reaction times and poor stereospecificities (Table 1, entries 2−6). Disappointingly, racemization and retrocycloaddition processes that compete with the isomerization were observed at temperatures higher than 35 °C, resulting in a decay of the asymmetric performance (Table 1, entries 7−8). The rearrangement also worked well at lower temperatures in terms of stereospecificity but with longer reaction times (Table 1, entry 9).

Isomerization in [60]Fulleropyrrolidines. Once optimized the experimental conditions for the enantiospecific *cis*−*trans* isomerization, we examined the scope of the reaction with respect to the electronic nature of substituents of the chiral [60]pyrrolidinofullerenes **2b−e** (Table 2, entries 1−18).

The isomerization worked very well for electron-releasing substituted pyrrolidinofullerenes **2b,c**, thus showing an excellent enantiocontrol and providing exclusively the corresponding stereoisomer with almost the same optical purity than the chiral starting cycloadduct (Table 2, entries 1−8). No differences were observed using either the *cis* or the *trans*

Scheme 2. Stepwise Isomerization Reaction Involving a Zwitterionic Intermediate

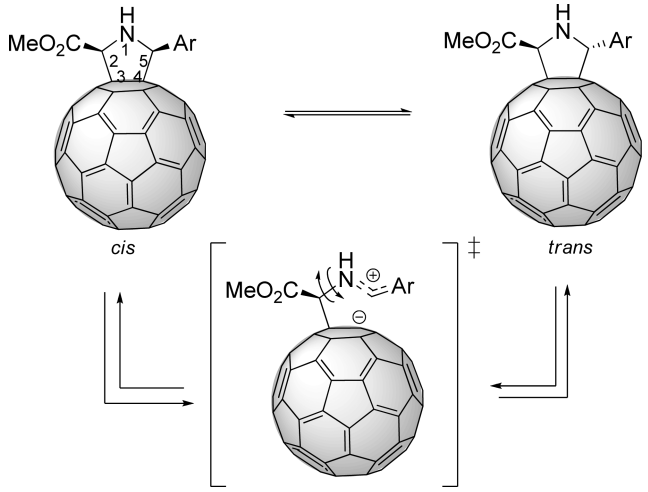

Table 2. Isomerization Reaction of Fulleropyrrolidines in 1-Chloronaphthalene:Acetonitrile 1:10 at 35°C

entry	starting derivative	*t* (d)	*cis*:*trans*[a]	ee *cis* (%)[b]	ee *trans* (%)[b]
1	*cis*-**2b**	0	99:1	90 (2*S*,5*R*)	–
2	*cis*-**2b**	7	68:32	88 (2*S*,5*R*)	87 (2*S*,5*S*)
3	*trans*-**2b**	0	1:99	–	90 (2*R*,5*R*)
4	*trans*-**2b**	7	70:30	84 (2*R*,5*S*)	84 (2*R*,5*R*)
5	*cis*-**2c**	0	99:1	90 (2*R*,5*R*)	–
6	*cis*-**2c**	6	71:29	89 (2*R*,5*R*)	89 (2*R*, 5*S*)
7	*trans*-**2c**	0	1:99	–	90 (2*R*,5*S*)
8	*trans*-**2c**	6	68:32	90 (2*R*,5*R*)	90 (2*R*,5*S*)
9	*cis*-**2d**	0	99:1	90 (2*S*,5*S*)	–
10	*cis*-**2d**	10	99:1	87 (2*S*,5*S*)	–
11	*trans*-**2d**	0	1:99	–	94 (2*S*,5*R*)
12	*trans*-**2d**	10	2:98	–	91 (2*R*,5*S*)
13	*cis*-**2e**	0	99:1	88 (2*S*,5*S*)	–
14	*cis*-**2e**	10	99:1	85 (2*S*,5*S*)	–
15	*trans*-**2e**	0	1:99	–	91 (2*S*,5*R*)
16	*trans*-**2e**	10	1:99	–	88 (2*R*,5*S*)
17[c]	*cis*-**2d**	10	83:17	65 (2*S*,5*S*)	64 (2*S*,5*R*)
18[c]	*cis*-**2e**	10	95:5	69 (2*S*,5*S*)	–
19	*cis*-**3**	0	99:1	96 (2*S*,5*R*)	–
20	*cis*-**3**	2	69:31	96 (2*S*,5*R*)	96 (2*S*,5*S*)
21	*cis*-**4**	0	99:1	94 (2*R*,5*S*)	–
22	*cis*-**4**	9	71:29	91 (2*R*,5*S*)	92 (2*S*,5*R*)
23	*cis*-**5a**	0	99:1	92 (2*S*,5*S*)	–
24	*cis*-**5a**	6	66:34	92 (2*S*,5*S*)	92 (2*S*,5*R*)
25	*cis*-**5a**	0	99:1	90 (2*R*,5*R*)	–
26	*cis*-**5a**	6	68:32	90 (2*R*,5*R*)	90 (2*R*,5*S*)
27	*trans*-**5a**	0	1:99	–	93 (2*S*,5*R*)
28	*trans*-**5a**	6	71:29	93 (2*S*,5*S*)	93 (2*R*,5*S*)

[a]Diastereoisomers ratio determined by crude ^{1}H NMR spectroscopy. [b]Enantiomeric excesses measured by chiral HPLC. [c]Reaction carried out at 60 °C.

derivative: the process was fully enantiospecific, reaching an equilibrium state with a mixture of both *cis* and *trans* products in ratios of about 70:30, respectively. Again, *cis* adducts **2b,c** resulted to be the products of thermodynamic control, whereas *trans* isomers are controlled by kinetics.

Pyrrolidinofullerenes **2d,e** bearing electron-withdrawing substituents did not exhibit the same behavior. None of them

DOI: 10.1021/ja5108854
J. Am. Chem. Soc. 2015, 137, 1190−1197

isomerized to the corresponding *cis* or *trans* adduct under the optimal experimental conditions (Table 2, entries 9−16). Higher temperatures were required, but even heating at 60 °C, *cis*-**2e** afforded only 5% of *trans*-**2e** after 10 days (Table 2, entry 18). On the other hand, the adduct bearing the *p*-fluorophenyl substituent *cis*-**2d** furnished 17% of *trans*-**2d** in 10 days at 60 °C (Table 2, entry 17). However, these low isomerizations were not enantiospecific, due to the high reaction temperature that favors the racemization and retrocycloaddition processes.

These experimental findings can be rationalized assuming a stepwise isomerization pathway that leads to a zwitterionic intermediate, stabilized by a fullerene anion and a benzylic cation, where the absolute configuration of the C2 from the pyrrolidine ring is already defined (Scheme 2). Thus, stable intermediates undergo rotation around the N−C2 pyrrolidine bond yielding the opposite diastereoisomer. It is interesting to note that, whereas the anion is the same for all the evaluated cycloadducts, the different stability of the benzylic cation will determine the outcome of the process. Consequently, highly stable electron-rich benzylic cations support the enantiospecificity in the isomerization of electron-rich aryl substituted fulleropyrrolidines. On the contrary, electron-withdrawing substituents on the aromatic ring results in a more energetically demanding reaction profile, thus requiring higher temperatures with a concomitant loss of chiral information (see Theoretical Calculations section).

Isomerization in [70]Fulleropyrrolidines. Encouraged by the excellent results achieved on C_{60}, we focused our attention in broadening the scope of this methodology to higher fullerenes, namely C_{70} as the most abundant and available higher fullerene. To our delight, the isomerization of 2-methoxycarbonyl-5-(2-thienyl)pyrrolidino[3,4:25′,8′][70]-fullerene (**3**), under the optimized conditions, proceeded in higher enantiospecificity and much faster than [60]-pyrrolidinofullerene (Scheme 3a). After 2 days, (2*S*,5*R*)-*cis*-**3** converted exclusively into the (2*S*,5*S*)-*trans*-**3** resulting in an equilibrium mixture of both *cis*-**3** and *trans*-**3** in a 7:3 ratio (Table 2, entries 19−20). Furthermore, the reaction achieved different levels of stereospecificity since no traces of other site- or regioisomers as isomerization byproducts were detected.

Scheme 3. Stereospecific *cis*−*trans* Isomerization in Enantiomerically Enriched [70]Fulleropyrrolidines 3 and 4

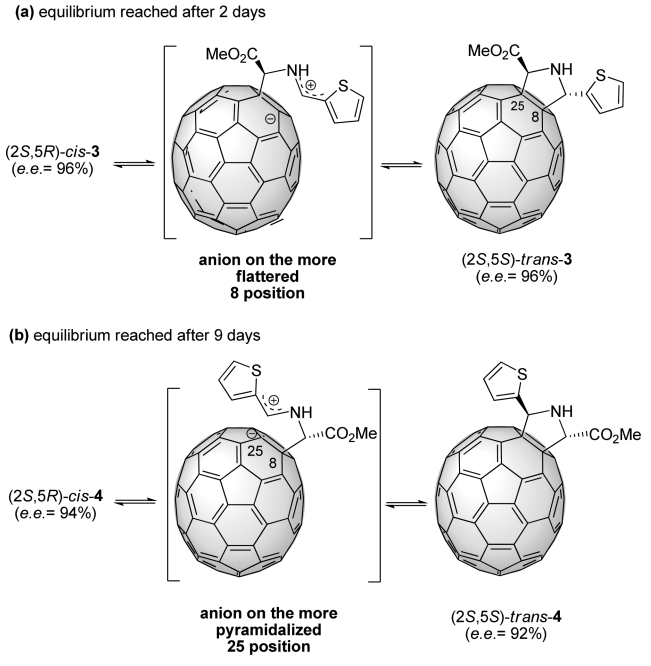

In contrast, regioisomer **4** bearing the ester moiety on the equatorial region of C_{70} did not perform in the same way (Scheme 3b). The *cis*−*trans* **4** isomerization, although enantiospecific, resulted to be much slower than for **3**, thus reaching the equilibrium state within 9 days (Table 2, entries 21−22).

In order to understand the origins of this different behavior observed for both regioisomers **3** and **4**, we should consider their zwitterionic intermediates. Indeed, the anion bent onto the C8 position of the C_{70} is more stable than the C_{60} anion due to the more planar geometry of the equatorial region.[8b] Therefore, a better performance in terms of stereospecificity and reaction rates can be expected for [70]pyrrolidinofullerenes isomerization. On the other hand, the intermediate involved in the *cis*−*trans*-**4** isomerization bears an anion located on the more curved polar region of the C_{70} molecule, resulting in a less stable intermediate (see Scheme 3). This difference of stability is consistent with the observed differences in the isomerization rates for both regioisomers.

Isomerization in Endohedral Fulleropyrrolidines. Endohedral fullerenes, since their discovery in 1990,[12] constitute a new class of carbon allotrope with an atom, molecule, or cluster inside the fullerene cage.[13] These singular molecules have been extensively used for a wide variety of purposes, involving material science[14] as well as medicinal chemistry.[15] Furthermore, endofullerenes represent an unusual, or even unique, setting from where it is also possible to carry out mechanistic insights of great value, as mentioned above.[7]

Given the inert character of the H_2 molecule incarcerated in the C_{60} cage,[11] we turned our attention to an endofullerene endowed with a polar water molecule incarcerated in the inner cavity, namely $H_2O@C_{60}$.[10a] In particular, we focused our study into chiral endofullerene derivatives **5a** endowed with a polar molecule (i.e., H_2O) inside the sphere. The *cis*−*trans* interconversion of **5a** enantiomers proved to be absolutely enantiospecific, furnishing the corresponding fulleropyrrolidines with excellent enantiocontrol (Table 2, even entries). Interestingly, we found that the reaction rates and enantiospecificities were slightly but persistently enhanced when compared with those obtained for the related empty-cage derivatives **2a**. These data suggest that the encapsulated water molecule is not inert and plays a significant role in the isomerization process.

To gain some insight into the endohedral influence on the reaction, kinetic experiments were conducted (Table 3). We carried out the isomerization using identical concentrations of chiral starting (2*S*,5*S*)-*cis*-**2a** and (2*S*,5*S*)-*cis*-**5a** under the previous optimal reaction conditions. The reaction was monitored using HPLC (see SI).

Although a reliable kinetic study is not possible due to the complexity of the *cis*−*trans* isomerization process (where retrocycloaddition reaction could also compete in some extent, thus affecting the kinetics), the plotting of C/Co vs time for **5a** and **2a** (Figure 3) shows a small but clear faster kinetics for endohedral **5a** with respect to the empty derivative **2a**.

Since all the reaction parameters are identical, the acceleration of the rearrangement in **5a** adducts could only be due to the incarcerated species influence. Actually, this different kinetic behavior could be rationalized by an unprecedented hydrogen bond assistance from a hydrogen

DOI: 10.1021/ja5108854
J. Am. Chem. Soc. 2015, 137, 1190−1197

Table 3. Comparison of Isomerization Reaction Rates of (2*S*,5*S*)-*cis*-2a and (2*S*,5*S*)-*cis*-5a in 1-Chloronaphthalene:Acetonitrile 1:10 at 35°C

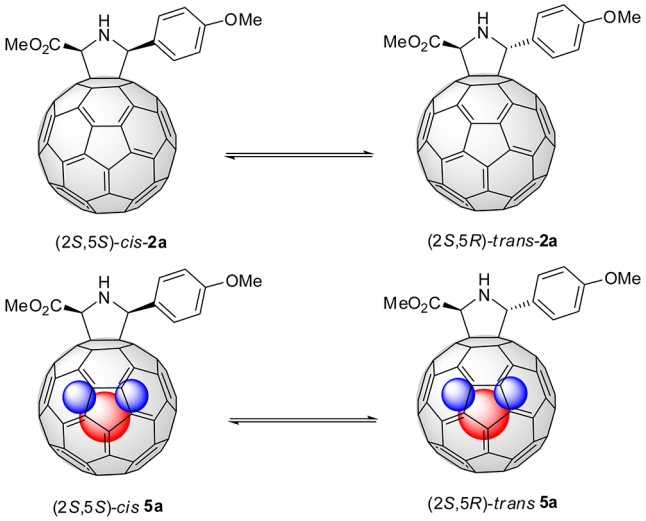

entry	starting derivative	*t* (d)	*cis*:*trans*[a]
1	*cis*-**2a**	0	99:1[b]
2	*cis*-**5a**	0	99:1[b]
3	*cis*-**2a**	1	99:1
4	*cis*-**5a**	1	97:3
5	*cis*-**2a**	2	98:2
6	*cis*-**5a**	2	95:5
7	*cis*-**2a**	3	92:8
8	*cis*-**5a**	3	87:13
9	*cis*-**2a**	4	85:15
10	*cis*-**5a**	4	78:22[b]
11	*cis*-**2a**	5	76:24[b]
12	*cis*-**5a**	5	71:29

[a]Diastereoisomers ratio determined by HPLC. [b]ee = 92.

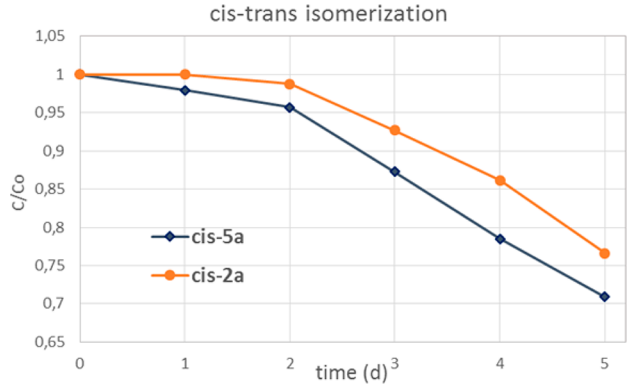

Figure 3. *Cis*–*trans* isomerization kinetics based on the data of Table 3. Time is expressed in days.

atom of the inner water molecule that provides an extra stabilization to the zwitterionic intermediate of the endohedral derivative (see below in the Theoretical Calculations). This nonpreviously observed interaction of the inner water molecule not only produces an enhancement of the isomerization rate but, in addition, also influences the stereochemical outcome.

Theoretical Calculations. We have performed DFT calculations at the M06-2X/6-311+G(d,p)//OLYP/TZP level of theory to unveil the mechanism of the isomerization process in the different cases studied experimentally (see SI for full computational details and references).[16] We have considered that the nitrogen inversion in the fulleropyrrolidines is a fast event (barrier of about 9 kcal/mol)[17] at the operating temperatures, and therefore, we have taken in all cases the most stable conformer. Our study starts with the investigation of the *cis*–*trans* isomerization in the C_{60}-based system **2a** and its possible competition with the retro-Prato reaction (see Figure 4). As anticipated from the experimental ratios obtained,

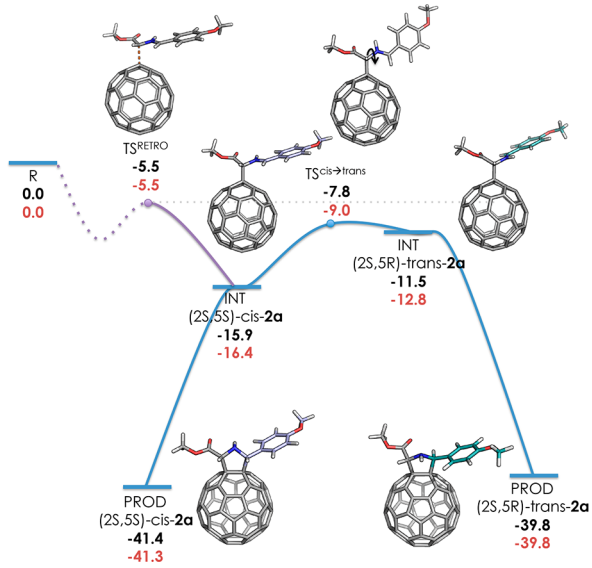

Figure 4. DFT mechanism for the *cis*–*trans* **2a** (black values) and the endohedral fulleropyrrolidine **5a** (red values) isomerization (represented using a blue line) and retro-Prato process (in purple). All energies are expressed in kcal/mol.

PROD-(2*S*,5*S*)-*cis* is ca. 1.6 kcal/mol more stable than the product PROD-(2*S*,5*R*)-*trans*. The lower stability of the *trans* product could be mainly attributed to the higher repulsion of the lone pairs of the nitrogen atom of the pyrrolidine ring and the carbonyl group of the ester substituent. The isomerization process takes place via a stepwise mechanism through the formation of two zwitterionic intermediates: INT(2*S*,5*S*)-*cis* and INT(2*S*,5*R*)-*trans* (see Figure 4). All attempts to find a biradical intermediate failed. This stepwise mechanism involving zwitterionic intermediates is in line with previous studies on 1,3-dipolar isomerization on endohedral metallofullerenes.[18]

In both cases, a fullerene anion and a benzylic cation is formed. DFT calculations indicate that the C–C bond dissociation process for the C5 position (benzyl electron donating group) presents a small activation of barrier of <1 kcal/mol, whereas the dissociation of the C2-position (ester, electron-withdrawing group) is highly unfavorable (see Figure S35). These results are in line with the fact that the absolute configuration of C2 is preserved along the isomerization process. INT(2*S*,5*S*)-*cis* and INT(2*S*,5*R*)-*trans* are ca. −16 and −12 kcal/mol more stable than isolated reactants. Once INT-*cis* has been formed, two possible pathways should be considered: (1) the *cis*–*trans* isomerization to achieve INT-*trans*, and (2) the retro-Prato process to recover the initial reactants. The most favorable isomerization process involves the rotation of the C2–N single bond and has an activation barrier of ca. 8 kcal/mol with respect to INT-*cis* (and of about 4 kcal/mol with

DOI: 10.1021/ja5108854
J. Am. Chem. Soc. 2015, 137, 1190–1197

respect to INT-*trans*). It should be emphasized that the isomerization process through the N−C5 bond is extremely unfavorable due to its higher double bond character (see Figure S36). In contrast, the retro-Prato reaction presents an activation barrier of ca. 10.5 kcal/mol. This is ca. 2.5 kcal/mol higher than the one corresponding to the *cis*−*trans* isomerization. These observations indicate that (1) the retro-Prato could compete with the isomerization process at high temperatures (as observed experimentally for instance in the cases **2d** and **2e**), and (2) the relative stability of the intermediate INT(2*S*,5*R*)-*trans* with respect to INT(2*S*,5*S*)-*cis* gives a reasonable estimate of the activation barrier of the isomerization process (<4.0 kcal/mol of difference between the activation barrier and relative stability of the *cis*−*trans* intermediates). In light of these observations, we decided to focus our study on the stabilities of the *cis* and *trans* intermediates for the rest of the considered cases.

The effect of the substituent, fullerene surface, and inner cluster on the isomerization process has been studied computationally (see Figure S37). In Table 4, the relative stabilities of *cis*−*trans* products and their respective intermediates for all studied systems are represented. In all cases, the *trans* product is ca. 1.5 kcal/mol less stable than the *cis* one, showing that the same *cis*−*trans* ratio will be obtained in all cases. As observed experimentally, the presence of electron-withdrawing groups in the benzyl substituent destabilizes the formed intermediates by approximately 2−3 and 5−6 kcal/mol for **2d** and **2e**, respectively (see Table 4). This substituent effect has been discussed previously for related species.[18] Under these conditions, the isomerization and retro-Prato reaction are both operative, which is in line with the experimental observations.

Table 4. M06-2X/6-311+G(d,p)//OLYP/TZP Relative Stabilities of *cis*−*trans* Products and Intermediates with Respect to Isolated Reactants for C_{60}, $H_2O@C_{60}$, and C_{70} Systems[a]

	C_{60}				$H_2O@C_{60}$	C_{70}	
	2a	**2d**	**2e**	**2b**	**5a**	**3**	**4**
PROD-*cis*	−41.4	−42.0	−41.1	−41.9	−41.3	−42.3	−42.1
INT-*cis*	−15.9	−13.3	−11.4	−14.8	−16.4	−19.0	−13.3
INT-*trans*	−11.5	−7.6	−3.0	−10.4	−12.8	−14.8	−8.6
PROD-*trans*	−39.8	−40.2	−39.4	−40.6	−39.8	−40.9	−40.8

[a]All energies in kcal/mol.

The effect of the fullerene surface has been investigated considering the bigger C_{70} fullerene. DFT calculations indicate that INT(2*S*,5*S*)-*cis*-**3** (−19.0 kcal/mol with respect to C_{70}+dipole) and INT(2*S*,5*R*)-*trans*-**3** (−14.8 kcal/mol) correspond to the most stable intermediates among all considered cases. In contrast, the corresponding intermediates for **4**, which bear the ester substituent on the equatorial region of C_{70}, are ca. 6 kcal/mol less stable than for **3** (−13.3 and −8.6 kcal/mol for INT-*cis* and INT-*trans*, respectively). For comparison, the relative stabilities of the latter thiophene-based intermediates in the case of C_{60} are −14.8 and −10.4 kcal/mol with respect to isolated reactants, respectively. The difference in reactivity for INT-(2*S*,5*S*)-*cis*-**2b**, **3**, and **4** can be rationalized by considering the average pyramidalization angle of the carbon atoms of the pentagonal ring where the new C−C bond is formed (10.0°, 10.8°, and 10.4° for **3**, **4**, and **2b**, respectively). In the most stable adduct **3** the negative charge is located in a more planar region, INT-*cis*-C_{60}-**2b** presents an intermediate pyramidalization angle, and the least planar geometry is found for the least stable C_{70}-**4**.

Finally, the effect on the isomerization process of having a water molecule in the fullerene inner cavity has been investigated (see Figure 5 and Table 4). Several orientations of the inner molecule have been considered (see Figure S38). By comparing the relative stabilities of both *cis* and *trans* endohedral intermediates with respect to the free cases, a slight stabilization of INT-*cis* (0.5 kcal/mol), but a substantial stabilization of INT-*trans* (ca. 1.3 kcal/mol) is observed for the H_2O molecule orientation leading to the most stable structure. As it can be seen in Figure 5, the inner water molecule is assisting the isomerization process by stabilizing the formed fullerene anion, where a hydrogen atom of the water molecule is directly pointing to the negatively charged carbon atom on fullerene surface. The distance between the hydrogen atom of the inner H_2O and the carbon atom where the addition will take place to form PROD-*trans* is ca. 2.7 Å in both *cis* and *trans* intermediates. The O−H distance in *cis* and *trans* intermediates is 0.967 Å, slightly elongated as compared to that in $H_2O@C_{60}$ (0.965 Å). In this latter species the C···HO interaction was classified as a weak H-bond in a previous work.[19] In *cis* and *trans* intermediates this H-bond is somewhat stronger. The H−C and O−H values in the *cis* and *trans* intermediates correspond to the usually observed H-bond distances, thus clearly showing that this H-bond stabilization is the main force that favors the isomerization process. It is important to mention that the inner water molecule has no effect on the final stability of the *cis* and *trans* products, neither on the retro-reaction pathway (see Table 4 and Figure 5). The activation barrier for the *cis*−*trans* isomerization is substantially lower in **5a** than in **2a** (7.4 and 8.1 kcal/mol for the endohedral

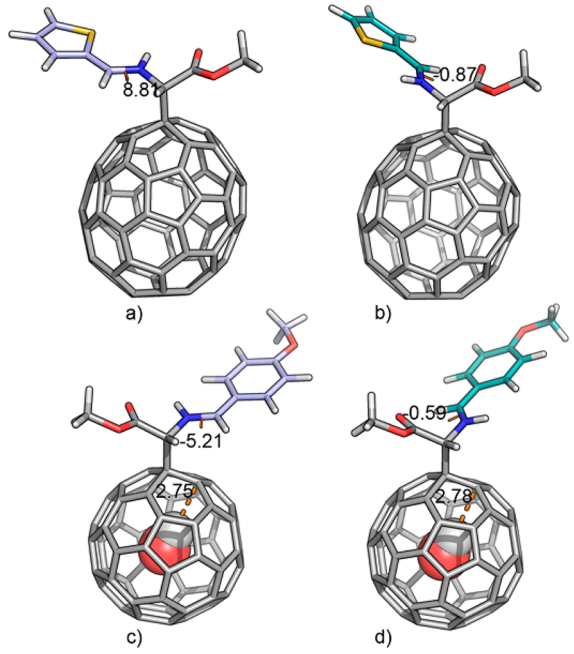

Figure 5. DFT optimized *cis*−*trans* intermediates for: (a) INT(2*S*,5*S*)-*cis*-**3**, (b) INT(2*S*,5*R*)-*trans*-**3**, (c) INT(2*S*,5*S*)-*cis*-**5a**, and (d) INT(2*S*,5*R*)-*trans*-**5a**. H_{H_2O}-C_{full} distance in angstroms and ∠CNCH dihedral angle in degrees.

DOI: 10.1021/ja5108854
J. Am. Chem. Soc. 2015, 137, 1190−1197

and free cage, respectively). This 0.7 kcal/mol of difference between activation barriers is in line with the improved stereochemical outcome observed experimentally for the endohedral fulleropyrrolidine case. Thus, the encapsulated H_2O molecule contributes to increase the isomerization rate without producing any change on the final *cis*–*trans* ratio or promoting the loss of chiral control through the retro reaction pathway.

CONCLUSIONS

In summary, we have described the first highly efficient and versatile asymmetric fullerene rearrangement. This novel unprecedented enantiospecific *cis*–*trans* isomerization in optically pure fulleropyrrolidines under mild conditions in polar solvents resulted to be effective with [60], [70], and endohedral fullerene ($H_2O@C_{60}$) derivatives. Furthermore, the isomerization result can be easily modulated at three different levels: out of the fullerene sphere, at the sphere, and inside it. Actually, a unique H-bonding assistance of polar molecules encapsulated inside fullerenes was observed, setting a precedent to the development of a novel "inner" manner to influence the stereochemical outcome in fullerene chemistry. Finally, DFT calculations completely account for the fully enantiospecific result of the isomerization and the relative stabilities of reaction intermediates, thus supporting the proposed stepwise mechanism. This work paves the way to the stereoselective control in further fullerene rearrangements and retrocycloaddition processes.

ASSOCIATED CONTENT

Supporting Information

General methods, synthesis of starting materials, spectroscopical data, computational methods and Cartesian coordinates of all stationary points located. This material is available free of charge via the Internet at http://pubs.acs.org.

AUTHOR INFORMATION

Corresponding Authors

*nazmar@quim.ucm.es
*salvatore.filippone@quim.ucm.es
*miquel.sola@udg.edu
*silvia.osuna@udg.edu

Notes

The authors declare no competing financial interest.

ACKNOWLEDGMENTS

Financial support by the European Research Council (ERC-320441-Chirallcarbon and FP7-PEOPLE-2013-CIG-630978 to S.O.), the Ministerio de Economía y Competitividad (MINECO) of Spain (projects CTQ2011-24652/BQU and CTQ2011-23156/BQU, JdlC contract to S.O., and AP2010-2517 to M.G.-B.), the CAM (PHOTOCARBON project S2013/MIT-2841), the Generalitat de Catalunya (project number 2014SGR931 and ICREA Academia 2009 to M.S.) is acknowledged. N.M. thanks to the Alexander von Humboldt Foundation.

REFERENCES

(1) (a) *Fullerenes: From Synthesis to Optoelectronic Properties*; Guldi, D. M., Martín, N.; Eds.; Kluwer: Dordrecht, Netherlands, 2002. (b) *Fullerenes: Chemistry and Reactions*, Hirsch, A., Brettreich, M.; Eds.; Wiley-VCH: Weinheim, 2005. (c) Martín, N.; Altable, M.; Filippone, S.; Martín-Domenech, A. *Synlett* **2007**, 3077.

(2) (a) Eiermann, M.; Wudl, F.; Prato, M.; Maggini, M. *J. Am. Chem. Soc.* **1994**, *116*, 8364. (b) Janssen, R. A.; Hummelen, J. C.; Wudl, F. *J. Am. Chem. Soc.* **1995**, *117*, 544. (c) Smith, A. B., III; Strongin, R. B.; Brard, L.; Furst, G. T.; Romanow, W. J.; Owens, K. G.; Goldschmidt, R. J.; King, R. C. *J. Am. Chem. Soc.* **1995**, *117*, 5492.

(3) (a) Kessinger, R.; Gómez-López, M.; Boudon, C.; Gisselbrecht, J. P.; Gross, M.; Echegoyen, L.; Diederich, F. *J. Am. Chem. Soc.* **1998**, *120*, 8545. For more information about Bingel cycloadducts, please see: (b) Bingel, C. *Chem. Ber.* **1993**, *126*, 1957. (c) Camps, X.; Hirsch, A. *J. Chem. Soc. Perkin Trans. 1* **1997**, 1595.

(4) (a) Cardona, C. M.; Elliott, B.; Echegoyen, L. *J. Am. Chem. Soc.* **2006**, *128*, 6480. (b) Rodríguez-Fortea, A.; Campanera, J. M.; Cardona, C. M.; Echegoyen, L.; Poblet, J. M. *Angew. Chem., Int. Ed.* **2006**, *45*, 8176.

(5) Tsuruoka, R.; Nagamachi, T.; Murakami, Y.; Komatsu, K.; Minakata, S. *J. Org. Chem.* **2009**, *74*, 1691.

(6) (a) Kessinger, J. R.; Crossous, J.; Herrmann, A.; Rüttimann, M.; Echegoyen, L.; Diederich, F. *Angew. Chem., Int. Ed.* **1998**, *37*, 1919. (b) Herranz, M. A.; Martín, N.; Ramey, J.; Guldi, D. M. *Chem. Commun.* **2002**, *38*, 2968. (c) Martín, N.; Altable, M.; Filippone, S.; Martín-Domenech, A.; Echegoyen, L.; Cardona, C. M. *Angew. Chem., Int. Ed.* **2006**, *45*, 110. (d) Herranz, M. A.; Diederich, F.; Echegoyen, L. *Eur. J. Org. Chem.* **2004**, 2299.

(7) (a) Ueno, H.; Kawakami, H.; Nakagawa, K.; Okada, H.; Ikuma, N.; Aoyagi, S.; Kokubo, K.; Matsuo, Y.; Oshima, T. *J. Am. Chem. Soc.* **2014**, *136*, 11162. (b) Yamada, M.; Ohkubo, K.; Shionoya, M.; Fukuzumi, S. *J. Am. Chem. Soc.* **2014**, *136*, 13240.

(8) (a) Filippone, S.; Maroto, E. E.; Martín-Domenech, A.; Suárez, M.; Martín, N. *Nat. Chem.* **2009**, *1*, 578. (b) Maroto, E. E.; de Cózar, A.; Filippone, S.; Martín-Domenech, Á.; Suárez, M.; Cossío, F. P.; Martín, N. *Angew. Chem., Int. Ed.* **2011**, *50*, 6060. (c) Maroto, E. E.; Filippone, S.; Martín-Domenech, A.; Suárez, M.; Martín, N. *J. Am. Chem. Soc.* **2012**, *134*, 12936. (d) Maroto, E. E.; Filippone, S.; Suárez, M.; Martínez-Álvarez, R.; de Cózar, A.; Cossío, F. P.; Martín, N. *J. Am. Chem. Soc.* **2014**, *136*, 705.

(9) (a) Marco-Martínez, J.; Marcos, V.; Reboredo, S.; Filippone, S.; Martín, N. *Angew. Chem., Int. Ed.* **2013**, *52*, 5115. (b) Marco-Martínez, J.; Reboredo, S.; Izquierdo, M.; Marcos, V.; López, J. L.; Filippone, S.; Martín, N. *J. Am. Chem. Soc.* **2014**, *136*, 2897.

(10) (a) Kurotobi, K.; Murata, Y. *Science* **2011**, *333*, 613. (b) Li, Y.; Lei, X.; Lawler, R. G.; Murata, Y.; Komatsu, K.; Turro, N. J. *Org. Lett.* **2012**, *14*, 3822. (c) Zhang, R.; Murata, M.; Wakamiya, A.; Murata, Y. *Chem. Lett.* **2013**, *42*, 879. (d) Krachmalnicoff, A.; Levitt, M. H.; Whitby, R. J. *Chem. Commun.* **2014**, *50*, 13037.

(11) Maroto, E. E.; Izquierdo, M.; Murata, M.; Filippone, S.; Komatsu, K.; Murata, Y.; Martín, N. *Chem. Commun.* **2014**, *50*, 740.

(12) (a) Krätschmer, W.; Lamb, L. D.; Fostiropoulos, K.; Huffman, D. R. *Nature* **1990**, *347*, 354. (b) Chai, Y.; Guo, T.; Jin, C.; Haufler, R. E.; Chibante, L. P. F.; Fure, J.; Wang, L.; Alford, J. M.; Smalley, R. E. *J. Phys. Chem.* **1991**, *95*, 7564.

(13) (a) Popov, A. A.; Yang, S.; Dunsch, L. *Chem. Rev.* **2013**, *113*, 5989. (b) Yamada, M.; Akasaka, T.; Nagase, S. *Acc. Chem. Res.* **2009**, *43*, 92. (c) Chaur, M. N.; Melin, F.; Ortiz, A. L.; Echegoyen, L. *Angew. Chem., Int. Ed.* **2009**, *48*, 7514. (d) Lu, X.; Feng, L.; Akasaka, T.; Nagase, S. *Chem. Soc. Rev.* **2012**, *41*, 7723. (e) Rodríguez-Fortea, A.; Balch, A. L.; Poblet, J. M. *Chem. Soc. Rev.* **2011**, *40*, 3551. (f) Garcia-Borràs, M.; Osuna, S.; Luis, J. M.; Swart, M.; Solà, M. *Chem. Soc. Rev.* **2014**, *43*, 5089. (g) Osuna, S.; Swart, M.; Solà, M. *Phys. Chem. Chem. Phys.* **2011**, *13*, 3585.

(14) (a) Kobayashi, S.; Mori, S.; Iida, S.; Ando, H.; Takenobu, T.; Taguchi, Y.; Fujiwara, A.; Taninaka, A.; Shinohara, H.; Iwasa, Y. *J. Am. Chem. Soc.* **2003**, *125*, 8116. (b) Yasutake, Y.; Shi, Z.; Okazaki, T.; Shinohara, H.; Majima, Y. *Nano Lett.* **2005**, *5*, 1057. (c) Tsuchiya, T.; Kumashiro, R.; Tanigaki, K.; Matsunaga, Y.; Ishitsuka, M. O.; Wakahara, T.; Maeda, Y.; Takano, Y.; Aoyagi, M.; Akasaka, T.; Liu, M. T. H.; Kato, T.; Suenaga, K.; Jeong, J. S.; Iijima, S.; Kimura, F.; Kimura, T.; Nagase, S. *J. Am. Chem. Soc.* **2008**, *130*, 450. (d) Ross, R.

DOI: 10.1021/ja5108854
J. Am. Chem. Soc. 2015, 137, 1190–1197

B.; Cardona, C. M.; Guldi, D. M.; Sankaranarayanan, S. G.; Reese, M. O.; Kopidakis, N.; Peet, J.; Walker, B.; Bazan, G. C.; Van Keuren, E.; Holloway, B. C.; Drees, M. *Nat. Mater.* **2009**, *8*, 208.
(15) (a) Cagle, D. W.; Kennel, S. J.; Mirzadeh, S.; Alford, J. M.; Wilson, L. J. *Proc. Natl. Acad. Sci. U.S.A.* **1999**, *96*, 5182.
(16) (a) Zhao, Y.; Truhlar, D. G. *Theor. Chem. Acc.* **2008**, *120*, 215. (b) Baker, J.; Pulay, P. *J. Chem. Phys.* **2002**, *117*, 1441.
(17) Lukoyanova, O.; Kitaygorodskiy, A.; Cardona, C. M.; Echegoyen, L. *Chem.—Eur. J.* **2007**, *13*, 8294.
(18) Aroua, S.; Garcia-Borràs, M.; Osuna, S.; Yamakoshi, Y. *Chem.—Eur. J.* **2014**, *20*, 14032.
(19) Varadwaj, A.; Varadwaj, P. R. *Chem.—Eur. J.* **2012**, *18*, 15345.

DOI: 10.1021/ja5108854
J. Am. Chem. Soc. 2015, 137, 1190−1197